TAL1-mediated regulation of hemocyte proliferation influences red blood phenotype in the blood clam Tegillarca granosa

Article · January 2024

CITATIONS
0

READS
23

5 authors, including:

Hongyu Jin
Ningbo University
9 PUBLICATIONS **20** CITATIONS
SEE PROFILE

Hongxing Liu
Zhejiang Wanli University
36 PUBLICATIONS **376** CITATIONS
SEE PROFILE

Aquaculture 586 (2024) 740801

Contents lists available at ScienceDirect

Aquaculture

journal homepage: www.elsevier.com/locate/aquaculture

TAL1-mediated regulation of hemocyte proliferation influences red blood phenotype in the blood clam *Tegillarca granosa*

Hongyu Jin [a,b], Hongxing Liu [a], Jiacheng Wang [a], Weiwei Zhang [b], Yongbo Bao [a,c,*]

[a] College of Biological & Environmental Sciences, Zhejiang Wanli University, Zhejiang 315100, China
[b] School of Marine Sciences, Ningbo University, Ningbo 315000, China
[c] Ninghai Institute of Mariculture Breeding and Seed Industry, Zhejiang Wanli University, Ningbo, 315604, China

ARTICLE INFO

Keywords:
TAL1
Tegillarca granosa
Hematopoiesis
Hemocyte proliferation
Red blood phenotype

ABSTRACT

Red blood phenotype, indicating the degree of red color in blood or hemolymph, is a significant economic trait in *Tegillarca granosa*, closely associated with its health condition and nutritive value. However, the molecular regulatory processes that account for the variation in the blood clams' red blood phenotype remain largely unexplored. In our previous studies, weighted gene co-expression network analysis (WGCNA) showed that *TAL1* exhibits high intramodular connectivity in red blood-related module. Furthermore, TAL1 serves as a critical transcription factor in the survival and quiescence of hematopoietic stem cells, along with being essential in the terminal maturation processes in vertebrates. Consequently, we investigated the function of the *TAL1* in blood clams by conducting a comparative analysis between high total hemocyte count (HTHC: THC $\geq 14 \times 10^4$ cells/μL) and low total hemocyte count (LTHC: THC $\leq 2.5 \times 10^4$ cells/μL) groups, as well as between negative control and Tg-TAL1 RNA interference groups of blood clams. The results revealed that, compared to LTHC group, there was a significant upregulation of *TAL1* mRNA and protein expression levels in the HTHC group, which may be a crucial factor contributing to the alterations observed in THC. RNA interference of the *TAL1* in blood clams resulted in a significant decline in THC, causing the blood color to become lighter. EdU staining experiments further confirmed a diminished cell proliferative vitality within *T. granosa* gills after *TAL1* knockdown. Moreover, immunohistochemical analysis and immunofluorescence assays revealed a gradual escalation in TAL1 protein expression and cytoplasmic/nuclear ratio from gill filament chamber endothelial cells to gill filament chamber cells in gills, potentially representing different cell types in the maturation process of erythrocytes in blood clams. It suggesting that the gills might act as one of the hematopoietic tissues in blood clams, with hemocytes potentially originating from the gill filament chamber endothelium of the gills through division and differentiation. This research improves comprehension of the molecular mechanisms behind the variation in *T. granosa*'s red blood phenotype, potentially assisting in the selective breeding of high THC *T. granosa* populations.

1. Introduction

Tegillarca granosa, a species of bivalve belonging to the family Arcidae, is colloquially known as the blood clam due to its distinctive red blood. It is primarily found in the Indo-Pacific region, inhabiting muddy or sandy substrates in estuarine and coastal environments, often in intertidal or shallow subtidal zones. Due to its robust and sweet flavor, *T. granosa* is highly esteemed and widely cultivated in Southeast Asian coastal countries such as Thailand and Malaysia, as well as in East Asian countries such as China and South Korea, reflecting its prominent status in both regional cuisine and aquaculture. Red blood phenotype specifically denotes the degree of red color of the blood or hemolymph, with hemoglobin concentration (HGC) and total hemocyte count (THC) serving as critical indicators of this phenotype (Jin et al., 2023a; Sun et al., 2022). Red blood phenotype reflects the health status of blood clams to some degree. In the same batch of blood clams, those with light-colored blood typically signify unhealthiness, potentially leading to reduced consumer interest in purchasing them (Yang et al., 2023). Furthermore, the extracted hemoglobin from blood clams shows significant potential in treating hypoferremia (Sun et al., 2022; Taniguchi et al., 2017). Moreover, erythrocytes and hemoglobin perform critical immune functions within blood clams. Hemoglobin of *T. granosa*

* Corresponding author at: Zhejiang Key Laboratory of Aquatic Germplasm Resources, College of Biological & Environmental Sciences, Zhejiang Wanli University, Zhejiang 315100, China.
E-mail address: baoyongbo@zwu.edu.cn (Y. Bao).

https://doi.org/10.1016/j.aquaculture.2024.740801
Received 25 January 2024; Received in revised form 1 March 2024; Accepted 8 March 2024
Available online 11 March 2024

contributes to the host antimicrobial defense through the peroxidase activity and certain peptides released from the proteins (Bao et al., 2013; Bao et al., 2016; Wang et al., 2021). Hemocytes in bivalves are capable of encapsulating pathogens and producing cytotoxic molecules, including reactive oxygen species, antimicrobial peptides, and inflammatory cytokines, which are involved in the killing and elimination of pathogens (Canesi et al., 2002; de la Ballina et al., 2022; Song et al., 2010).

In vertebrates, HGC is the major factor responsible for the redness of blood, with higher concentrations correlating with deeper blood coloration (Ali et al., 2022; Hu et al., 2021; Outman et al., 2023; Shibata et al., 2012). Multiple factors can influence the expression of hemoglobin. In humans, the suppression of *BCL11A* expression in primary adult erythroid cells induces a significant increase in fetal hemoglobin (HbF) expression (Michelson, 2008; Sankaran et al., 2010). Furthermore, the application of RNA interference (RNAi) and overexpression to modulate *CBFA2T3* levels in human primary erythroblasts demonstrated that *CBFA2T3* significantly inhibits the expression of *HBB*, *HBA*, and *ALAS2* (Fujiwara et al., 2013; McDonough et al., 2012; Steinauer et al., 2017). The Locus Control Region is the critical component governing beta-globin genes (*HBE1*, *HBG2*, *HBG1*, *HBD*, and *HBB*) expression, primarily enhancing their transcription by interacting with their promoters to facilitate the recruitment of transcription factors and the creation of an active chromatin configuration (Debnath et al., 2017; Nain et al., 2022; Sun et al., 2017). However, the genetic basis and molecular pathways driving red blood phenotype formation in blood clams remain unclear, particularly in comparison to vertebrates. Consequently, it is imperative to investigate the genetic underpinnings of this phenotype to provide a basis for the selective breeding of *T. granosa* with deep blood coloration. In our previous research, it was observed that the upregulation or downregulation of certain genes in *T. granosa*, such as *CBFA2T3* and *CDC42*, which play key roles in hemocyte differentiation regulation, affects the red blood phenotype (Jin et al., 2023a; Yang et al., 2023).

TAL1 (T cell acute lymphocytic leukemia 1), also known as SCL or TCL5, is a critical transcription factor involved in hematopoiesis and leukemogenesis processes (Rojas-Sutterlin et al., 2014; Tan et al., 2019; Toscano et al., 2015; Vagapova et al., 2018). A crucial role of TAL1 lies in sustaining the potential of hematopoietic stem cells to differentiate into multiple cell types while maintaining their state in the cell cycle G0 phase (Anantharaman et al., 2011; Chagraoui et al., 2018; Rojas-Sutterlin et al., 2014). Research has demonstrated that administering the T-ALL UTX inhibitor to human TAL1-positive blast cells effectively diminishes their proliferation rate and induces apoptosis (Benyoucef et al., 2016). The knockout of TAL1 significantly inhibited proliferation of monocytes differentiated from human common myeloid precursor cells and reduced the entry into and traversal through the G1 and S phases (Dey et al., 2010). Additionally, TAL1 forms significant SCL complexes with multiple transcription factors, such as E2A/HEB, RUNX1, LMO1/2, CBFA2T3, ERG/FLI1, Ldb1 and GATA1/2/3 (Hoang et al., 2016; Vagapova et al., 2018; Yamada et al., 2022). These complexes are integral in regulating myeloid lineage differentiation, managing erythroid precursor cells proliferation, and influencing the direction of hematopoietic stem cells differentiation pathways (Leong et al., 2017; Mansour et al., 2013; Ryan et al., 2007; Yamada et al., 2022). Beyond its role in normal hematopoietic processes, the SCL complex is also implicated in the malignant transformation of blood cells, suggesting its potential involvement in leukemic pathogenesis (Palii et al., 2011; Vagapova et al., 2018). Nevertheless, prior investigations have primarily concentrated on humans and mammals, while the function of the TAL1 gene in invertebrates, especially in bivalves, has yet to be elucidated. In preliminary research, through weighted gene co-expression network analysis (WGCNA), it was discovered that *Tg-TAL1* gene exhibits high intramodular connectivity in red blood-related module of *T. granosa*, suggesting *Tg-TAL1* might have a pivotal role in the formation of the red blood phenotype (Jin et al., 2023a).

In the current study, we employed quantitative real-time PCR (qRT-PCR) and western blotting techniques to examine the expression levels of mRNA and protein of *Tg-TAL1* in *T. granosa* populations, characterized by high and low THC. Immunohistochemistry was used to determine the localization pattern of Tg-TAL1. Additionally, RNA interference technology was utilized to further investigate the impact of the *Tg-TAL1* gene on the red blood phenotype and cell proliferative vitality in *T. granosa*. This research provides new perspectives on how the *TAL1* gene affects red blood phenotype of blood clams, laying a foundation for genetic breeding related to this distinct trait.

2. Materials and methods

2.1. Conserved domain and motif, protein tertiary structure and phylogenetic analysis

TAL1 sequences of *Homo sapiens*, *Mus musculus*, *Xenopus laevis*, *Alligator sinensis*, *Gallus gallus*, and *Danio rerio* were searched and downloaded from UniProt (https://www.uniprot.org/; last accessed on October 14, 2023). Moreover, the genome data of *Tegillarca granosa*, *Mytilus galloprovincialis*, *Mizuhopecten yessoensis*, *Crassostrea gigas*, *Sepia pharaonis*, *Capitella teleta*, *Biomphalaria glabrata*, *Aplysia californica*, *Drosophila melanogaster*, and *Lytechinus variegatus* were obtained from the NCBI database (last accessed on October 20, 2023), and eggnog-mapper v2.1.12 was used to identify TAL1 sequences from these species. For the methodologies pertaining to domain and motif prediction, as well as three-dimensional structure prediction of TAL1 sequences, refer to the reference (Jin et al., 2023b).

In the study, we employed the *E*-INS-I strategy for aligning TAL1 sequences utilizing MAFFT v7.463 (Rozewicki et al., 2019). MrBayes v3.2.7a was used to perform phylogenetic analysis through Bayesian inference (Ronquist et al., 2012). This process involved running four Markov chains over 100,000 generations, with samples collected at intervals of 1000 generations. Following this, iTOL v6 (Letunic and Bork, 2021) was used for a deeper analysis of the trees obtained from Bayesian analysis. To enhance the visual comprehension of the evolutionary relationships among TAL1 sequences in diverse species, silhouettes sourced from PhyloPic (https://www.phylopic.org/; last accessed on November 15, 2023) was employed.

2.2. Cloning, expression, purification of the recombinant Tg-TAL1 and preparation of rabbit antibodies

Full-length cDNA of Tg-TAL1 was codon-optimized for expression in *E. coli* (Fig. S1). Subsequently, codon-optimized DNA sequence was commercially synthesized (Genscript, Nanjing, China) and cloned into pET-30a (+). *Sma*I and *Hin*dIII were utilized to verify the plasmid's usability (Fig. 2a). The plasmid was then transformed into *E. coli* BL21 (DE3). Positive clones, confirmed by colony-based PCR, were chosen for large-scale production and purification.

The conditions required to induce the expression of rTg-TAL1 proteins refer to the reference (Wu et al., 2020). The bacteria were harvested by centrifugation at 12000 rpm for 10 min, followed by resuspending the resulting cell pellet in PBS buffer (5 mL PBS buffer was added per gram of cell pellet). A portion of the bacterial culture was processed using JY92-IIN ultrasonic cell crusher (Xin Yi Co., Ltd., Jiangsu, China) and the supernatant and precipitate were collected separately. To confirm the successful expression of rTg-TAL1, the bacterial culture, supernatant, and precipitate were each separately subjected to SDS-PAGE (Fig. 2b). Western blotting was employed to confirm the expression of rTg-TAL1 in supernatant (Fig. 2c).

Recombinant protein was purified using AKTAprime™ PLUS Protein Purification System (GE, America) and a Ni-NTA column (6FF His, 5 mL). First, the supernatant was loaded into Ni-NTA column pre-equilibrated with washing buffer 1 (Contains 500 mM NaCl and 20 mM Tris-HCl, pH = 7.9). Secondly, the column was eluted using a gradient of washing buffer 1 and washing buffer 2 (washing buffer 2

contained 500 mM imidazole, 500 mM NaCl and 20 mM Tris-HCl, pH = 7.9) a at a flow rate of 0.5 mL/min. By setting "Length" parameter to 50 mL and "Target" parameter to 100%, the gradient will gradually change the proportion of washing buffer 1 from 100% to 0%, and increase washing buffer 2 from 0% to 100% during the elution process. During this process, the concentration of imidazole in the Ni-NTA column will increase from 0 mM to 500 mM. Thirdly, elution was monitored at 280 nm and fractions were collected according to absorbance peaks (Fig. S2a). Finally, fractions that were collected underwent analysis using SDS-PAGE (Fig. S2b).

Antibodies were synthesized by HuaAn Biotechnology Co., Ltd. (Hangzhou, China). For the study, prime New Zealand White rabbits (~2.5 kg) were selected. The choice of animals was based on their healthy appearance, characterized by a lustrous coat and free movement. Selected animals were pre-conditioned for about two weeks to exclude any that might not meet the criteria, ensuring the smooth progression of subsequent experiments. The antigen(1 mg/mL), thoroughly mixed, was administered for immunization, with each rabbit receiving a dose of 0.5 mL. The antigen dosage was halved for the second to fourth immunizations. Adjuvants were prepared in a 1:1 volume ratio with the antigen. The primary immunization used complete adjuvant, while the subsequent ones used incomplete adjuvant. During extraction, the adjuvant was thoroughly mixed before being drawn into the syringe. The rabbits were immunized via multiple subcutaneous injections, each injection being 0.2 mL. The immunization schedule involved a second immunization on the 14th day following the primary immunization and subsequent immunizations at 7-day intervals. Serum samples for antibody detection were collected from the auricular artery of the rabbits 7 days after the third immunization. If the tests were satisfactory, a booster immunization was administered 7 days later, and whole blood was collected 7 days after the booster. The serum was purified using affinity chromatography, and all antibodies were combined and concentrated using ultrafiltration. The concentrated antibodies were then dialyzed in 1 L PBS buffer at room temperature, changing the solution every 3 h, for a total of three changes. Finally, 0.22 μm low protein binding filters were utilized to filter the dialyzed antibodies. The concentration of these antibodies was measured using a DeNovix DS-11 spectrophotometer on the Protein A280 application.

For the collection of serum samples, the experimental rabbit was restrained in a fixing frame. The ear was gently tapped to dilate the central artery. The area was disinfected with 75% alcohol, and while the left hand held the rabbit's ear, the right hand used a syringe to draw blood from the central artery about one-third from the tip, parallel to the artery, and towards the heart. Up to 8 mL of blood was collected at a time, followed by pressing with a cotton ball to stop the bleeding. For whole blood collection, the required immunized rabbits were first caught and their ear tag numbers checked before being weighed. They were then anesthetized intravenously with 1 mL/kg of 3% sodium pentobarbital. After anesthesia, the rabbits were positioned with their abdomens up and limbs secured on a stainless-steel mesh frame, and blood was collected using the cardiac puncture method. The blood-filled centrifuge tubes were then placed in a 37 °C for 30 min before cooling and storing in a 4 °C refrigerator. After the blood naturally separated into layers, supernatant was transferred to 50 mL centrifuge tubes. Subsequently, the mixture was centrifuged at 12000 rpm for 2 min, and then supernatant was transferred into clean tubes. To the 50 mL of supernatant, 100 μl of 10% sodium merthiolate solution was added (final concentration 0.02%), mixed well, and stored at −20 °C. Detection of the potency of rabbit anti-rTg-TAL1 antibodies at different dilutions using ELISA (Table S1).

2.3. Determining HTHC and LTHC groups based on THC

Approximately 300 *T. granosa* individuals (10.7–12.5 g, two years old) were collected from a local aquaculturist's pond in Ningbo City, Zhejiang Province, China. These clams were then maintained under regulated environmental conditions with temperatures and salinity levels held at 25.32 ± 0.53 °C and 25.64 ± 0.86‰, respectively. For the methodology of feeding blood clams, it is advisable to consult the reference (Jin et al., 2023b). Post a week of consistent cultivation, clams that were healthy, indicated by their standard blood color and quick stress response, were picked for ensuing studies. The specific criteria for selecting blood clams are as follows: First, when the blood clams naturally open their shell, observe the blood inside their mantle. Blood clams that neither presented a pale coloration nor exhibited evident clotting in the blood within their mantle were selected. Subsequently, a sterile plastic dropper is gently used to touch the foot of the blood clam. If the blood clam can rapidly retract its foot and close its shell, it is deemed to be in a healthy state.

In the initial phase of the study, a cohort of 100 healthy clams was carefully selected, from which approximately 500 μL blood was methodically extracted using a pipette (Eppendorf, Germany). Blood was collected by piercing the clam's mantle with a micropipette equipped with a yellow tip, which has a maximum capacity of 200 μL, followed by gentle aspiration of the blood and its transfer into a sterile 2 mL centrifuge tube. Subsequently, extract 10 μL blood and dilute it 100-fold with PBS buffer. This mixture was gently homogenized, and a 10 μL sample was transferred to a hemocytometer. THC was ascertained using a microscope (Olympus, Japan). The clams were categorized based on their THC: the three samples exhibiting the highest THC of blood were designated as the HTHC group, and those showing the lowest THC of blood were assigned to the LTHC group (Fig. S3). In the final step, gill tissues were harvested from three clams each from the HTHC and LTHC groups. For each group, one gill tissue sample from three different clams (noting that each clam has two gill tissues) was reserved and stored at −80 °C.

Details regarding the methodology for qRT-PCR are available in our previously published work (Jin et al., 2023b). Table S2 lists the specific primers used in this study.

2.4. RNAi of Tg-TAL1 and identification of proliferative cells

In vivo gene knockdown was executed utilizing siRNA-mediated RNAi targeting the Tg-TAL1 gene to elucidate the influence of Tg-TAL1 on THC. Following a week-long acclimatization period, each of the three groups was assigned six healthy blood clams. Upon addition of ddH_2O to the siRNA lyophilized powder, the concentration of siRNA was maintained at 20 μM. The baseline group (time 0 h) comprised clams that received no injection. The experimental group, designated as the Tg-TAL1 interference group, included clams injected with Tg-TAL1 siRNA solution. Conversely, the clams of negative control group injected with non-targeting siRNA solution, as detailed in Table S2.

Subsequent to the injection, at both 72 and 96 h, three clams from both experimental and control groups were selected for THC and HGC analysis. The phenotypic characteristics of the blood were meticulously documented through photography, and gill tissue samples were extracted from these clams using the aforementioned method for further examination. Specifically, at 72 h post-interference, gills from the two groups of clams were utilized for immunohistochemistry experiments. At 96 h post-interference, gills from the two groups were subjected to EdU staining experiments.

In EdU staining experiments, gill tissues from both Tg-TAL1 interference and negative control groups were cultured in DEME medium, containing 1% penicillin-streptomycin solution and 10 mM EdU, for a duration of 12 h. During the cultivation of gill tissues, CO_2 concentration was sustained at 5% and temperature held constant at 37 °C. Post-cultivation, these tissues were transferred to glass bottles with 4% neutral paraformaldehyde for fixation over a 24-h period.

The fixed tissue samples were subjected to a sequential dehydration protocol using ethanol solutions of increasing concentrations. This process involved treatment with 75% ethanol for 4 h, 85% ethanol for 2 h, 90% ethanol for 1.5 h, and 95% ethanol for 1.5 h, followed by two

successive 0.5-h treatments with anhydrous ethanol. Subsequently, the dehydrated gill tissues were treated with a 1:1 mixture of anhydrous ethanol and xylene for 10 min, followed by two 10-min treatments with xylene alone. The tissues were then sequentially immersed in three grades of paraffin wax, each with different melting points (54 °C, 56 °C, and 60 °C), to ensure thorough infiltration. Finally, the tissues were encased in paraffin wax with a 60 °C melting point and sectioned using a LEICA RM2125RT microtome (Leica, Germany) for further histological analysis.

These sections were subjected to a dewaxing procedure and subsequently stained with Yefluor 488 Azide Mix, facilitating the labeling of EdU with a fluorescent dye. Nuclear counterstaining was executed using Hoechst dye. Stained sections were photographed with fluorescence microscope (Nikon, Japan).

2.5. Western blotting

For this procedure, 20 mg of gill tissue was lysed in 1 mL of RIPA lysis buffer (Biodragon, China) and incubated for 30 min before centrifugation at 12,000 rpm for 10 min. A total of 100 ng of gill tissue protein was separated via 4–20% SDS-PAGE and subsequently transferred onto a polyvinylidene difluoride (PVDF) membrane at 400 mA for 30 min. The membrane was then blocked in PBST containing 5% skimmed milk at 37 °C for 1 h. After that, the membrane incubated with rabbit anti-rTg-TAL1 antibodies, diluted by this blocking solution (1500), at 4 °C for 12 h. Wash three times for 10 min each using PBST. Subsequently, the membrane underwent three PBST washes and were incubated with horseradish peroxidase (HRP)-conjugated goat anti-rabbit IgG(H + L) (Proteintech, China), diluted by blocking solution (12000), at 37 °C for 1 h. Through a further three washes in PBST, the membrane was visualized using Enhanced Chemiluminescent (NCM Biotech, China) and the Amersham Imager 600 (GE, America). The optical density values of the bands were estimated using ImageJ v2.15.0 (Schindelin et al., 2012).

2.6. Localization of Tg-TAL1 in gills using immunohistochemistry and immunofluorescence

In immunohistochemistry experiments, gill tissues were fixed using 4% neutral paraformaldehyde. The method for preparing tissue sections has been previously described. The deparaffinization of the sections was carried out as follows: the sections were first baked in a 60 °C incubator for 60 min, followed by two 15-min immersions in xylene. To rehydrate, the sections were sequentially immersed in anhydrous ethanol, 95%, 85%, and 75% ethanol (each for 5 min), and finally in ddH_2O for 5 min.

Antigen retrieval was performed using citrate buffer in a pressure cooker for 4 min, followed by natural cooling to room temperature and two subsequent 5-min soaks in ddH_2O. The sections were then washed twice with ddH_2O and three times with immunostaining washing buffer (Sangon, China) for 5 min each.

The tissue samples on the slides were circled using an immunohistochemistry hydrophobic pen, and 3% H_2O_2 in methanol was applied for 15 min. Subsequently, the sections underwent three 5-min washes using the immunostaining washing buffer. The sections were then blocked with immunostaining blocking solution (Sangon, China) for 45 min. Rabbit anti-rTg-TAL1 antibodies diluted 1:400 in PBST were applied and incubated at 4 °C for 12 h. This was succeeded by four 5-min washes using immunostaining washing buffer. HRP-conjugated goat anti-rabbit IgG(H + L) (Proteintech, China) was then applied and incubated at 37 °C for 1 h, succeeded by four 5-min washes with immunostaining washing buffer. Diaminobenzidine (DAB) chromogen was prepared and applied to the sections for color development in a humidified chamber, followed by termination of the reaction with distilled water. Hematoxylin staining solution was applied to each tissue for 10 min, then rinsed off with ddH_2O. The sections were decolorized in 1% hydrochloric acid in ethanol for 15 s, immediately transferred to distilled water to stop the reaction, and then placed in PBST (around pH 7.4) for 5–10 min to blue the nuclei.

Finally, the sections were sequentially soaked in 75%, 85%, 95% and 100% ethanol, each for 5 min, followed by two 15-min immersions in xylene. The sections were then mounted with a neutral resin cover slip. Images were captured using an OLYMPUS BX53 microscope. ImageJ v2.15.0 was employed for the calculation of mean optical density (MOD) values.

In immunofluorescence experiments, the methodology for acquiring gill tissue and the production of paraffin sections has been previously described. After dewaxing the sections using the same method, the sections were subsequently immersed in a sodium citrate solution (2.94 g/L) at a temperature of 95 °C for a duration of 20 min. Subsequently, the sections were treated with a blocking solution, composed of 5% fetal bovine serum and 0.3% Triton X-100 in PBS buffer, and incubated at room temperature for 1 h. After the application of Rabbit anti-rTg-TAL1 antibodies, diluted at a 1:500 ratio in blocking solution, the sections were incubated overnight at 4 °C.

The sections were washed with PBST for 10 min, a process that was repeated thrice. Subsequently, FITC-labeled goat anti-rabbit antibodies (Proteintech, China), diluted at a 1:500 ratio with the blocking solution, were applied to the sections and incubated at room temperature for 1 h. The sections were again washed with PBST for 10 min, a procedure repeated three times. Following this, the sections were treated with DAPI solution (10 ng/mL) for 10 min. Finally, images were captured using fluorescence microscope (Nikon, Japan).

3. Results

3.1. Characterization and evolutionary analysis of TAL1 in T. granosa and other species

A phylogenetic analysis of TAL1 sequences from 16 species, including *T. granosa*, was conducted using Bayesian methods, with the results integrated with predictions of conserved domains and motifs (Fig. 1a). The results show that vertebrates forming one major group, with subgroups reflecting the common ancestries of mammals, birds and reptiles, amphibians, and fish. TAL1 sequences of *H. sapiens* and *M. musculus* are closely related on the tree, reflecting their shared mammalian heritage. *A. sinensis* and *G. gallus*, both archosaurs, cluster together, with their TAL1 sequences likely more akin to each other than to those of mammals or lower vertebrates, reflective of their shared evolutionary origin.

Conversely, mollusks constitute a separate major group with potential subgroups corresponding to various classes, such as bivalves (blood clams, mussels, scallops, and oysters), gastropods (snails), and cephalopods (cuttlefish), demonstrating a marked evolutionary divergence in their TAL1 sequences from those of vertebrates. Among other invertebrates, the annelid *C. teleta* exhibits a closer evolutionary connection to mollusks, while the insect *D. melanogaster* and the echinoderm *L. variegatus* display a more distant evolutionary relationship with vertebrates.

Moreover, in humans, the TAL1 protein's basic helix-loop-helix (bHLH) domain has the capability to bind DNA, thereby exerting transcriptional functions. And all TAL sequences have conserved bHLH domains (Fig. 1a-c), which suggests that other TAL1 proteins, including Tg-TAL1, are likely to perform functions similar to those of TAL1 of *H. sapiens*.

3.2. Expression and purification of rTg-TAL1

The pET-30a-Tg-TAL1 (Fig. 2a, lane 1) plasmid was characterized through digestion and sequencing analysis. Post digestion with *Sma*I and *Hin*dIII, fragments of the expected sizes, 4957 bp and 1242 bp, were obtained (Fig. 2a, lane 2), confirming the successful construction of the pET-30a-Tg-TAL1 vector. The additional bands observed in lane 1, besides the expected 6199 bp, are likely attributed to the supercoiling and

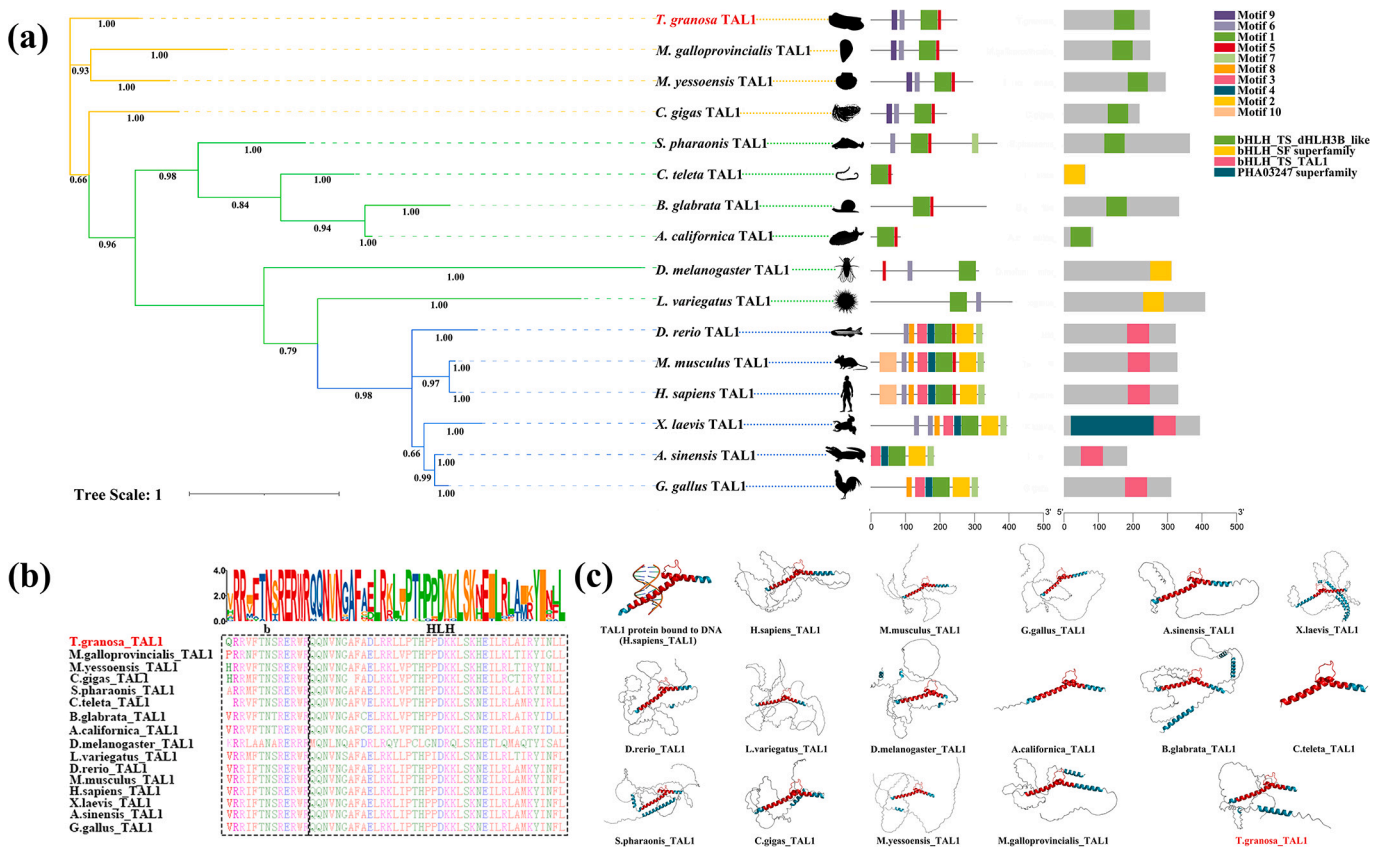

Fig. 1. Characterization and evolutionary analysis of TAL1 proteins in sixteen species. (a) Domain and motif analysis of TAL1 proteins, complemented by a phylogenetic analysis using the Bayesian inference method. Branches in blue represent vertebrates, those in yellow denote bivalve mollusks, and green branches symbolize other invertebrates. (b) Multiple sequence alignment analysis of the conserved domains of TAL1 proteins. (c) The 3D structures of TAL1 proteins are predicted using AlphaFold2, with the selection of the best model as recommended by the software. The bHLH structural domain is highlighted in red. (For interpretation of the references to color in this figure legend, the reader is referred to the web version of this article.)

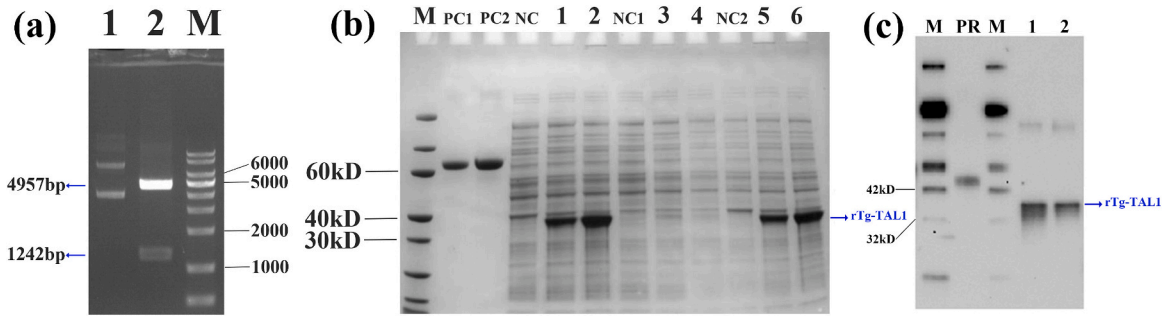

Fig. 2. Cloning, expression and purification of rTg-TAL1 in *E. coli* BL21. (a) Digestion analysis of the constructed plasmid pET-30a-Tg-TAL1 in 1% agarose. Lane M, 10000 bp DNA marker; Lane 1, undigested plasmid; Lane 2, plasmid digested by restriction enzymes *Sma*I and *Hin*dIII. (b) SDS-PAGE analysis of protein from *E. coli* BL21 following induction at 37 °C for 4 h and 15 °C for 16 h. Lane M, protein marker; Lane PC1: BSA (1 μg); Lane PC2: BSA (2 μg); Lane NC: cell lysate without induction; Lane 1: cell lysate with induction for 16 h at 15 °C; Lane 2: cell lysate with induction for 4 h at 37 °C; Lane NC1: supernatant of cell lysate without induction; Lane 3: supernatant of cell lysate with induction for 16 h at 15 °C; Lane 4: supernatant of cell lysate with induction for 4 h at 37 °C; Lane NC2: pellet of cell lysate without induction; Lane 5: pellet of cell lysate with induction for 16 h at 15 °C; Lane 6: pellet of cell lysate with induction for 4 h at 37 °C. (c) Western blotting of supernatant of cell lysate with induction at 37 °C for 4 h and 15 °C for 16 h. Lane M: protein marker; Lane PR: His-tagged positive reference protein; Lane 1: supernatant of cell lysate with induction for 16 h at 15 °C; Lane 2: supernatant of cell lysate with induction for 4 h at 37 °C.

linearization of the plasmid.

Following IPTG induction, pET-30a-Tg-TAL1 was successfully expressed in *E. coli* cells. Ultrasonic disruption of cells, induced at 15 °C for 16 h and at 37 °C for 4 h, and subsequent SDS-PAGE analysis (Fig. 2b) revealed the expression of rTg-TAL protein in both supernatant and inclusion bodies under both induction conditions, with an approximate molecular weight of 38 kD. Moreover, under 15 °C induction for 16 h, the expression level of rTg-TAL protein was approximately 15 mg/L, with a solubility of about 5%. Western blotting further confirmed the expression of rTg-TAL1 protein (Fig. 2c). The rTg-TAL1 protein was successfully purified using a linear imidazole gradient elution, identifying the optimal imidazole concentration for elution as 85 mM (Fig. S2a-b).

3.3. The upregulation of mRNA and protein expression of Tg-TAL1 in HTHC group

Consistent with expectations, blood clams in HTHC group exhibited markedly deeper blood coloration and higher HGC compared to those in LTHC group (Fig. 3a). To investigate the potential biological function of *Tg-TAL1* in *T. granosa*, both protein and mRNA expression levels of the *Tg-TAL1* were analyzed in the gills of HTHC and LTHC groups. The results indicated a significant upregulation of *Tg-TAL1*, both at mRNA and protein levels, in HTHC group (Fig. 3b-d, Fig. S4a).

3.4. The decline in both THC and HGC accompanied by a discernible lightening of blood color after knockdown of Tg-TAL1

To further elucidate the impact of the *Tg-TAL1* gene on the red blood phenotype, we employed Tg-TAL1-specific siRNA to knock down the *Tg-TAL1* gene, and the reduction in *Tg-TAL1* gene expression was confirmed at mRNA and protein levels (Fig. 4a-c, Fig. S4b). The results indicated that, at 72- and 96-h post-interference with the *Tg-TAL1* gene, there was a notable decline in THC and HGC (Fig. 4d-e). Additionally, a noticeable lightening in the color of the clam blood was observed following the *Tg-TAL1* gene interference (Fig. 4a).

3.5. Cell proliferative vitality declined after knockdown of Tg-TAL1

To ascertain the impact of *Tg-TAL1* on the cell proliferative vitality of *T. granosa*, we conducted EdU staining experiments following the knockdown of *Tg-TAL1*. As depicted in Fig. 5, compared to negative control group, Tg-TAL1 interference group displayed fewer EdU-stained nuclei. This disparity in the quantity of EdU-stained nuclei was consistently detected across various samples when comparing Tg-TAL1 interference group with control group, which suggests that interference with the *Tg-TAL1* gene diminishes the cell proliferative vitality in *T. granosa* gills.

These findings illuminate the significant role of the *Tg-TAL1* gene in regulating hematopoiesis and hemocyte proliferation in *T. granosa*.

3.6. Characterization of Tg-TAL1 protein expression in gills

To deepen our understanding of Tg-TAL1, we employed immunohistochemistry for its localization. The cell nuclei were stained blue with hematoxylin. Tissues containing Tg-TAL1 protein, after being bound by

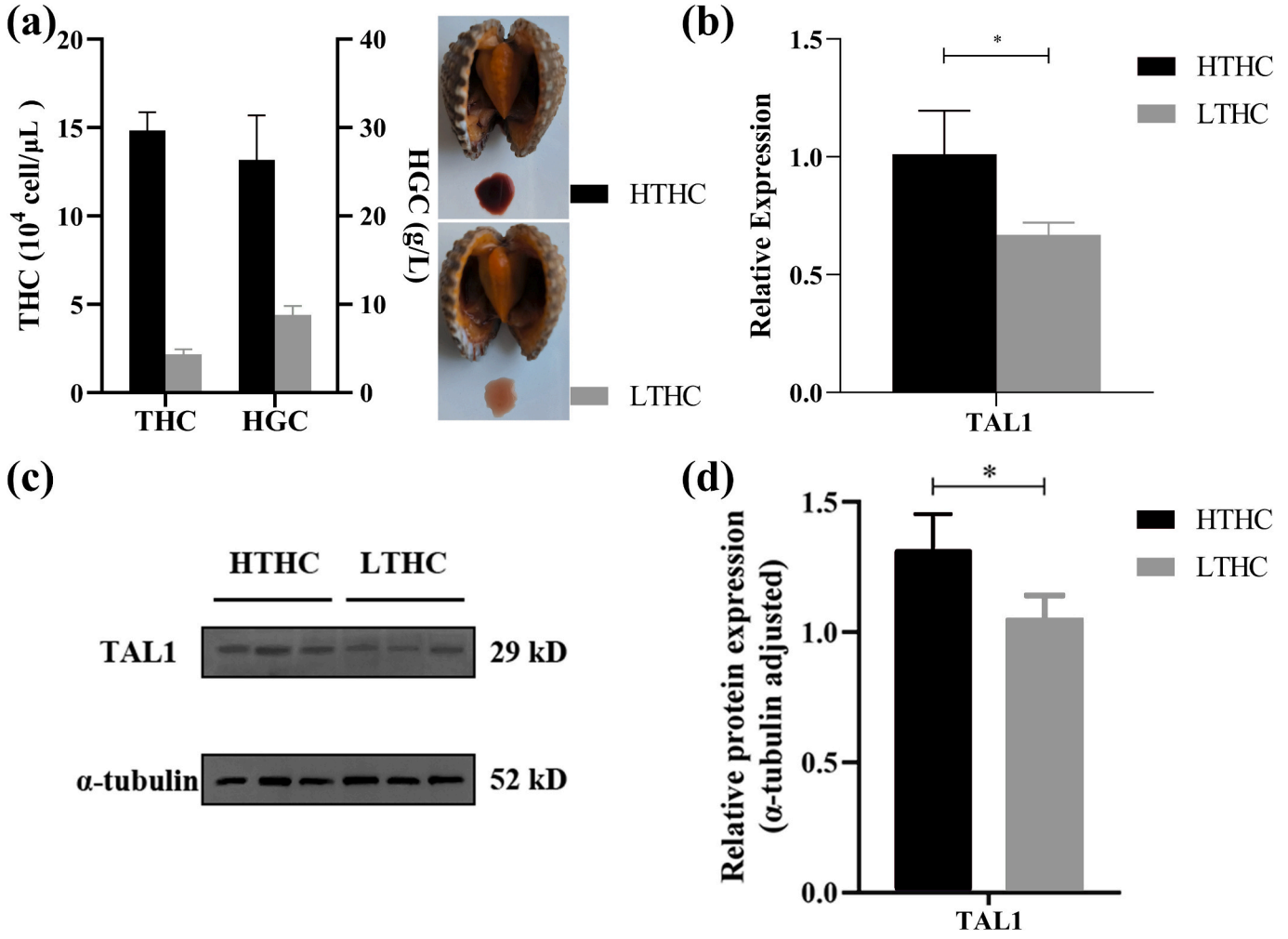

Fig. 3. The red blood-related traits of the high total hemocyte count (HTHC) and low total hemocyte count (LTHC) groups were analyzed, along with the relative quantification of *Tg-TAL1* mRNA and protein expression levels in the gill tissues of these groups using quantitative real-time PCR (qRT-PCR) and western blotting. (a) There were observed differences in red blood-related traits and variations in the red blood phenotype, between the HTHC and LTHC groups. (b) Relative quantification of mRNA levels of *Tg-TAL1* in the gill tissues of the HTHC and LTHC groups was performed using qRT-PCR. (c) Western blotting was employed to detect the expression of TAL1 and α-tubulin proteins in the gill tissues of the HTHC and LTHC groups. (d) The relative quantification of Tg-TAL1 protein levels in the gill tissues of the HTHC and LTHC groups was conducted. ImageJ was utilized for the quantification of the grayscale values of the bands obtained from western blotting results. (For interpretation of the references to color in this figure legend, the reader is referred to the web version of this article.)

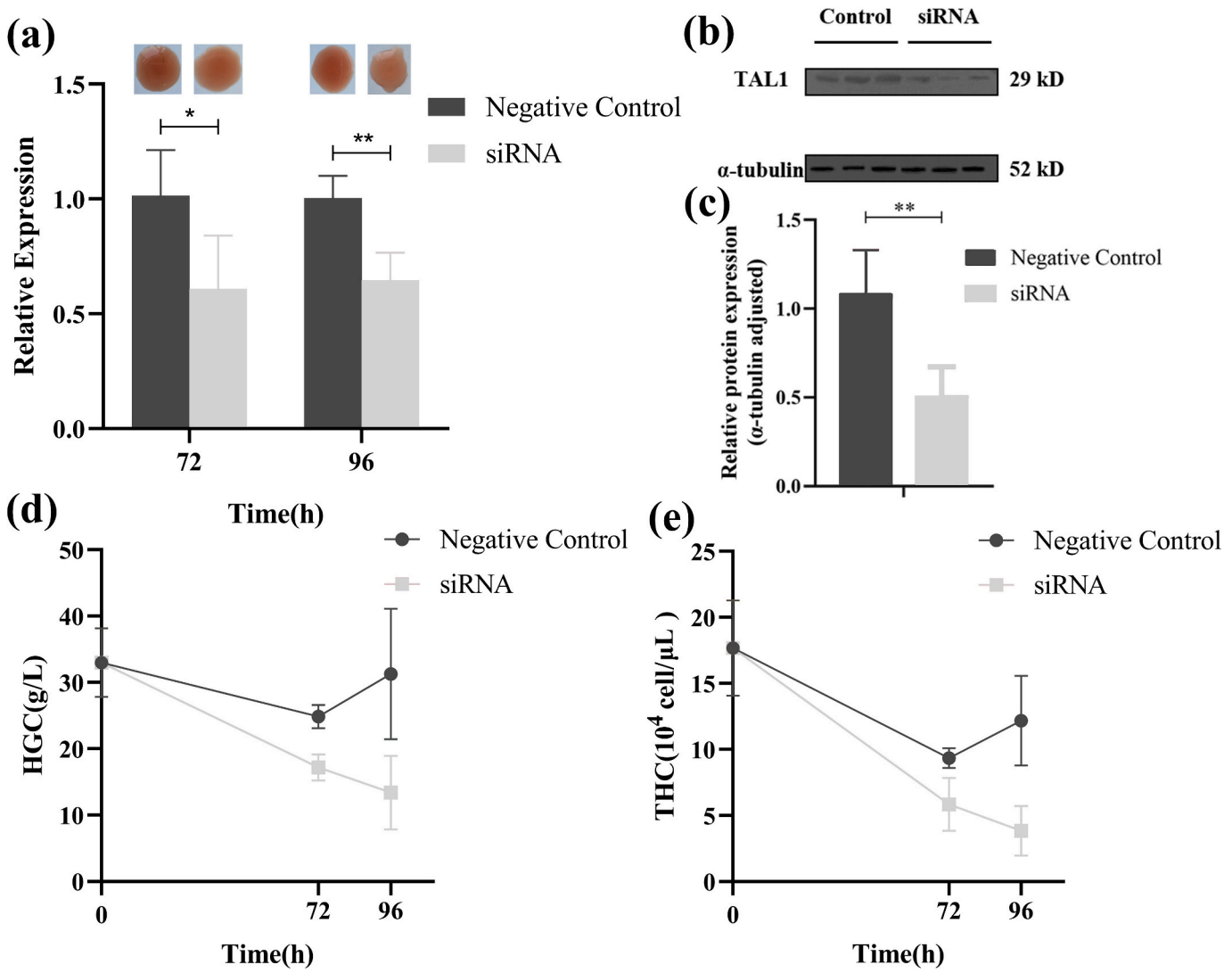

Fig. 4. Variations in red blood-related traits were observed at 72 and 96 h post RNA interference of *Tg-TAL1*. qRT-PCR (a) and western blotting (b-c) were utilized to relatively quantify the mRNA and protein levels of *Tg-TAL1* in blood clams of both negative control group and Tg-TAL1 RNA interference group. Changes in HGC (d) and THC (e) were noted following 72 and 96 h of RNAi targeting *Tg-TAL1*. (For interpretation of the references to color in this figure legend, the reader is referred to the web version of this article.)

rabbit antibodies against rTg-TAL1, were stained brown with DAB, with areas of darker brown indicating higher concentrations of Tg-TAL1 protein. The results revealed that within the gill filaments, most cells in the gill filament chambers were stained dark brown, while gill filament chamber endothelial cells exhibited only light brown staining, indicating a predominant expression of Tg-TAL1 protein in hemocytes. Moreover, the expression levels of Tg-TAL1 protein in gill filament chamber cells exhibit notable variations: Tg-TAL1 protein tends to be expressed at lower levels in cells with lesser cytoplasm and at higher levels in cells with abundant cytoplasm. Among these, cells with lesser cytoplasm exhibit varying degrees of adhesion to gill filament chamber endothelial cells, seemingly indicative of their transition from gill filament chamber endothelial tissues into the gill filament chamber (Fig. 6a). Moreover, in immunofluorescence assays, a more intense green fluorescence signifies higher expression levels of Tg-TAL1 protein. Immunofluorescence assays reveals that cells with a larger cytoplasmic/nuclear ratio exhibit stronger green fluorescence, indicating a higher expression of Tg-TAL1 protein in these cells (Fig. 7).

Notably, Tg-TAL1 protein was primarily expressed in the nucleus and cytoplasm, which may relate to its function as a transcription factor (Fig. 6a, Fig. 7). Furthermore, in line with expectations, gill tissue sections from the HTHC group displayed lower MOD values compared to the LTHC group, suggesting a greater presence of Tg-TAL1 protein in the gills of the HTHC group of *T. granosa* (Fig. 6b, Fig. S5). In accordance with the results from protein relative quantification, compared to negative control group, gills in Tg-TAL1 interference group also exhibited significantly lower MOD values (Fig. 6c, Fig. S5).

4. Discussions

TAL1 is a crucial transcription factor that plays a pivotal role in the survival and quiescence of adult hematopoietic stem cells, as well as in the terminal maturation of select blood lineages (Hung et al., 2021; Porcher et al., 2017; Vagapova et al., 2018). Phylogenetic analysis indicates that Tg-TAL1 is evolutionarily closest to the TAL1 genes of bivalves (Mg-TAL1, My-TAL1, and Cg-TAL1), and more distantly related to vertebrate orthologs. The bHLH domain mediates the formation of dimeric protein complexes and engages with *E*-box elements (CANNTG) of target genes, thereby modulating the transcription of these genes (Anantharaman et al., 2011; El Omari et al., 2013; Zhang et al., 2021). As Fig. 1 shows, Tg-TAL1 shares a highly conserved bHLH domain and a similar three-dimensional structure with other orthologs. This suggests

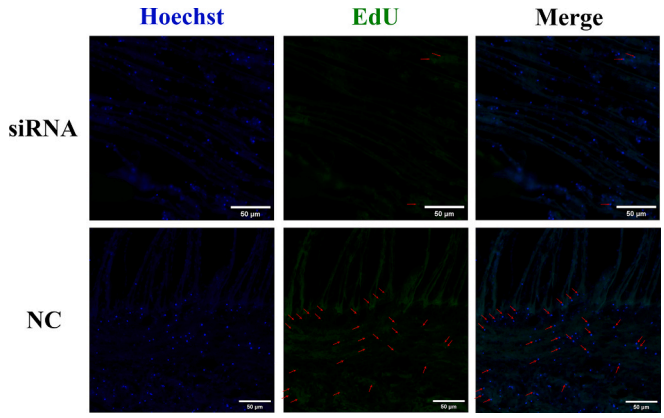

Fig. 5. Fluorescence microscopy was employed to examine gill tissue sections, which were co-stained with Hoechst and EdU. Hoechst stain was applied for DNA binding to signify the location of the nucleus, whereas EdU, indicated by a red arrow, was used to label replicated DNA. Gill sections from Tg-TAL1 interference group displayed a reduced number of nuclei with green fluorescence, suggesting a diminished cell proliferative vitality. (For interpretation of the references to color in this figure legend, the reader is referred to the web version of this article.)

that the *Tg-TAL1* gene may share functional similarities with the human *TAL1* gene, including the regulation of hematopoietic cell proliferation and differentiation. Interestingly, in previous studies, we constructed a red blood-related module using WGCNA, wherein *Tg-TAL1* exhibited high intramodular connectivity. This further suggests the significant role of *Tg-TAL1* in the development of red blood phenotype. Consequently, we investigated the function of the *Tg-TAL1* gene in blood clams by conducting a comparative analysis between HTHC and LTHC groups, and also between negative control and Tg-TAL1 RNA interference groups of blood clams.

Overexpression of TAL1 inhibits the expression of the mTOR pathway suppressor gene *DDiT4*, thereby enhancing the proliferation of human umbilical hematopoietic stem cells (Benyoucef et al., 2015). To investigate the potential influence of the *Tg-TAL1* gene on hemocyte proliferation in *T. granosa*, we employed qRT-PCR and western blotting for relative quantification of *Tg-TAL1* mRNA and protein expression levels in HTHC and LTHC groups. The results revealed a significant upregulation of both mRNA and protein expression of *Tg-TAL1* in HTHC group compared to LTHC group. This suggests that the upregulation of the *Tg-TAL1* gene may be a significant factor contributing to the increased THC in *T. granosa* populations, potentially as a result of TAL1's role in enhancing hemocyte proliferation (Benyoucef et al., 2015; Song et al., 2016).

The initial discovery of RNA interference occurred when exogenous dsRNA was injected into *Caenorhabditis elegans*, leading to the silencing of homologous endogenous mRNAs (Fire et al., 1998). Currently, RNA interference is considered a powerful tool in the study of gene function and is widely employed in the investigation of gene functionality in mollusks (Clark et al., 2020; Fan et al., 2024; Gu et al., 2022; Yu et al., 2023). To further explore the effects of down-regulation of *Tg-TAL1* on red blood phenotype of *T. granosa*, we carried out RNA interference experiments targeting *Tg-TAL1*. Subsequently, we found that blood clams displayed a notable decline in THC and HGC, along with a discernible lightening of blood color after RNA interference of *Tg-TAL1* gene. Moreover, a significant decrease in the count of EdU-stained nuclei was observed in Tg-TAL1 interference group, suggesting that RNA interference of *Tg-TAL1* significantly impacts the cell proliferative vitality in *T. granosa*.

To date, research into the hematopoietic sites and mechanisms in bivalves remains insufficiently explored. In prior research, gills have been identified as the primary hematopoietic tissues in *Crassostrea gigas* (Jemaà et al., 2014; Song et al., 2019) and *Chlamys farreri* (Zhang et al., 2023). Furthermore, in the irregularly folded structures of the adult gills of *Crassostrea gigas*, it has been discovered that hemocytes can differentiate from clusters of adult somatic cells (Jemaà et al., 2014), with stem cells undergoing division and differentiation into prohemocytes within the gills (Jia et al., 2021). Recently, our laboratory has identified genes that may regulate stem cell differentiation, including *CDC42*, *Sox2*, and *Sox9*, along with hematopoiesis-related genes like *RUNX1* and *GATA2*, which exhibit heightened mRNA expression levels in gill tissues. (Yang et al., 2023). Additionally, results from WGCNA have also indicated that the gills display characteristics significantly associated with the red blood-related module (Jin et al., 2023a). Immunofluorescence assays indicate that during the process of human angiogenesis, TAL1 protein is maintained at a high level of expression in primitive erythrocytes and at a low level in surrounding endothelial cells (Drake and Fleming, 2000; Hoang et al., 2016). Similarly, immunohistochemical analysis and immunofluorescence assays revealed a relatively low level of Tg-TAL1 protein expression in the gill filament chamber endothelial cells of the gills, while varying degrees of expression are observed within the gill filament chamber cells of the gills. Within the gill filament chamber, cells expressing lower levels of Tg-TAL1 protein often have smaller cytoplasm and some of them exhibit adhesion to the gill filament chamber endothelium. Interestingly, the cytoplasmic/nuclear ratio (Yan et al., 2021) and TAL1 protein expression level (Goardon et al., 2006; Hoang et al., 2016) of human erythroid progenitor cells also increases during progressive maturation. Consequently, the gills might serve as one of the hematopoietic tissues in blood clams, potentially even as the primary site, where hemocytes could originate through division and differentiation from the gill filament chamber endothelial tissues of the gills.

Beyond *TAL1*, *CBFA2T3*, as a member of the TAL1 complex, has also been demonstrated to play a significant role in the formation of red blood phenotype of blood clams (Jin et al., 2023a). Consequently, given the unique nature of blood clams as bivalves possessing hemoglobin and red blood cells, it merits to investigate the existence of a complex in blood clams that is similar to the human TAL1 complex, functioning to regulate the hemocyte proliferation and terminal differentiation. Future research will explore the interactions of components in TAL1 complex of blood clams. It will also elucidate the molecular processes by which the TAL1 complex affects the proliferation and differentiation of hemocytes. Moreover, the gradual differentiation of progenitor cells into erythrocytes in blood clams, whether this process originates in the gill tissues, and in which tissues these cells mature, are questions that warrant further in-depth investigation.

Interestingly, in contrast to the blood clams, which possess only a single form of the TAL1 protein sequence (248 aa), humans have two isoforms of the TAL1 protein: TAL1-l (331 aa) and TAL1-s (156 aa) (Calkhoven et al., 2003; Hoang et al., 2016; Vagapova et al., 2018). The pre-mRNA of human TAL1 is alternatively spliced to produce mRNA lacking certain exons, leading to a translation product, the TAL1-s protein, which lacks the CBFA2T3-binding domain and phosphorylation sites but retains the DNA-binding domains and bHLH domain (Xu et al., 2017). TAL1-s is required for erythroid progenitor cells differentiation, while TAL1-l is required for megakaryocytic progenitor cells differentiation (Vagapova et al., 2018). Therefore, it warrants further investigation whether the Tg-TAL1 protein, with a sequence length intermediate between TAL1-l and TAL1-s, possesses the CBFA2T3-binding domain and phosphorylation sites, and what role it plays in the differentiation process of erythrocytes.

5. Conclusion

In conclusion, *Tg-TAL1* may influence the red blood phenotype of *T. granosa* by regulating hemocyte proliferation. Initially, within a blood clam population, a marked upregulation in mRNA and protein levels of *Tg-TAL1* was detected in high THC group compared to low THC group. Subsequently, we demonstrated the critical role of *Tg-TAL1* in regulating

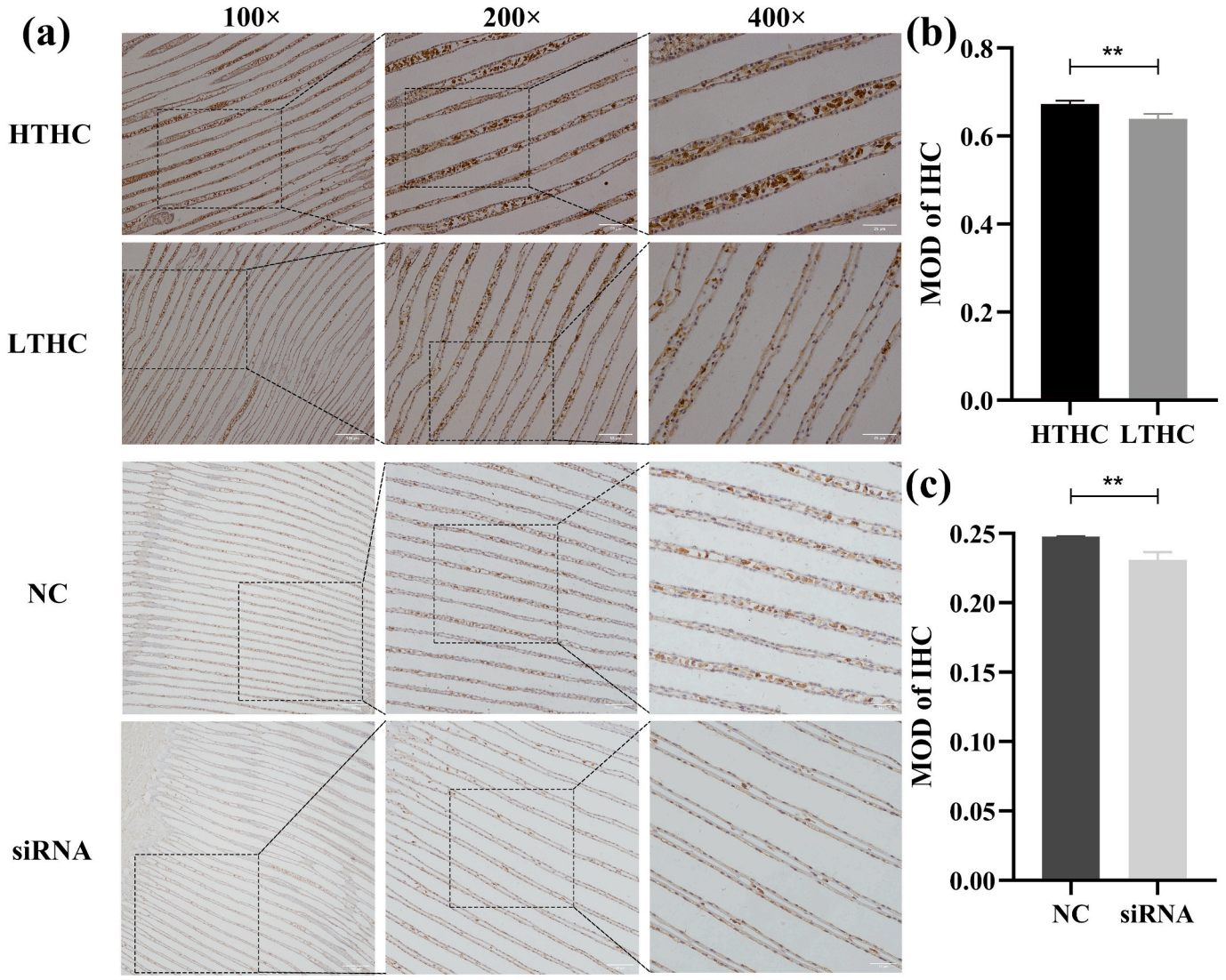

Fig. 6. The localization of Tg-TAL1 in the gill tissues of blood clams was investigated using immunohistochemistry (IHC). (a) IHC was employed to localize Tg-TAL1 in the gill tissues of blood clams across different groups: HTHC group, LTHC group, negative control group (NC), and Tg-TAL1 RNA interference group (siRNA). (b) The mean optical density (MOD) values of the immunohistochemical sections of gill tissues were measured for both HTHC and LTHC groups. (c) The MOD values of the immunohistochemical sections from negative control group and Tg-TAL1 RNA interference group were also quantified. The MOD values represent the intensity of the brown coloration in the sections, which to a certain extent, can be indicative of the expression levels of the Tg-TAL1 protein. ImageJ was utilized for the quantitative analysis of MOD values in the immunohistochemical sections. (For interpretation of the references to color in this figure legend, the reader is referred to the web version of this article.)

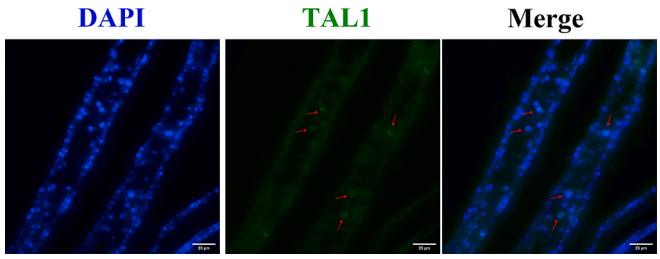

Fig. 7. The localization of Tg-TAL1 in the gill tissues of blood clams was investigated using immunofluorescence (IF) assays. DAPI was applied for DNA binding to signify the location of the nucleus. Tg-TAL1 protein shows green fluorescence when indicated by antibodies labeled with FITC. Red arrows were used to indicate cells with high TAL1 protein expression. (For interpretation of the references to color in this figure legend, the reader is referred to the web version of this article.)

hematopoiesis, significantly affecting the red blood phenotype of blood clams by RNA interference and EdU staining. Finally, immunohistochemical analysis and immunofluorescence assays indicated a gradual increase in the protein expression of *Tg-TAL1* and cytoplasmic/nuclear ratio from gill filament chamber endothelial cells to gill filament chamber cells in gills, potentially representing different cell types during the erythrocyte maturation process in *T. granosa*. It suggesting that the gills might serve as one of the hematopoietic tissues in blood clams, with hemocytes potentially arising from the gill filament chamber endothelium of the gills through division and differentiation. This study provides crucial evidence for the impact of up- or down-regulation of *Tg-TAL1* on red blood phenotype of blood clams and lays a foundation for unraveling the molecular mechanisms behind the variations in red blood phenotype.

CRediT authorship contribution statement

Hongyu Jin: Writing – original draft, Visualization, Investigation.

Hongxing Liu: Resources, Investigation. **Jiacheng Wang:** Data curation. **Weiwei Zhang:** Data curation. **Yongbo Bao:** Writing – review & editing, Project administration.

Declaration of competing interest

The author declares that he has no conflict of interests.

Data availability

The data underlying this article are available in the article and in its online supplementary material.

Acknowledgments

This work was financially supported by the National Science Foundation of China (32273123), the Ningbo Public Benefit Research Key Project (2021S014), the Zhejiang Major Program of Science and Technology (2021C02069-7) and the Key Natural Science Foundation of Ningbo (2023J042).

Appendix A. Supplementary data

Supplementary data to this article can be found online at https://doi.org/10.1016/j.aquaculture.2024.740801.

References

Ali, A., Soman, S.S., Vijayan, R., 2022. Dynamics of camel and human hemoglobin revealed by molecular simulations. Sci. Rep.-Uk 12 (1), 122. https://doi.org/10.1038/s41598-021-04112-y.

Anantharaman, A., Lin, I.J., Barrow, J., Liang, S.Y., Masannat, J., Strouboulis, J., Huang, S.M., Bungert, J., 2011. Role of Helix-loop-Helix proteins during differentiation of erythroid cells. Mol. Cell. Biol. 31 (7), 1332–1343. https://doi.org/10.1128/mcb.01186-10.

de la Ballina, N.R., Maresca, F., Cao, A., Villalba, A., 2022. Bivalve Haemocyte subpopulations: a review. Front. Immunol. 13, 826255 https://doi.org/10.3389/fimmu.2022.826255.

Bao, Y., Li, P., Dong, Y., Xiang, R., Gu, L., Yao, H., Wang, Q., Lin, Z., 2013. Polymorphism of the multiple hemoglobins in blood clam Tegillarca granosa and its association with disease resistance to Vibrio parahaemolyticus. Fish Shellfish Immunol. 34 (5), 1320–1324. https://doi.org/10.1016/j.fsi.2013.02.022.

Bao, Y., Wang, J., Li, C., Li, P., Wang, S., Lin, Z., 2016. A preliminary study on the antibacterial mechanism of Tegillarca granosa hemoglobin by derived peptides and peroxidase activity. Fish Shellfish Immunol. 51, 9–16. https://doi.org/10.1016/j.fsi.2016.02.004.

Benyoucef, A., Calvo, J., Renou, L., Arcangeli, M.L., van den Heuvel, A., Amsellem, S., Mehrpour, M., Larghero, J., Soler, E., Naguibneva, I., Pflumio, F., 2015. The SCL/TAL1 transcription factor represses the stress protein DDiT4/REDD1 in human hematopoietic stem/progenitor cells. Stem Cells 33 (7), 2268–2279. https://doi.org/10.1002/stem.2028.

Benyoucef, A., Palii, C.G., Wang, C., Porter, C.J., Chu, A., Dai, F., Tremblay, V., Rakopoulos, P., Singh, K., Huang, S., Pflumio, F., Hébert, J., Couture, J.-F., Perkins, T.J., Ge, K., Dilworth, F.J., Brand, M., 2016. UTX inhibition as selective epigenetic therapy against TAL1-driven T-cell acute lymphoblastic leukemia. Genes Dev. 30 (5), 508–521. https://doi.org/10.1101/gad.276790.115.

Calkhoven, C.F., Müller, C., Martin, R., Krosl, G., Hoang, T., Leutz, A., 2003. Translational control of SCL-isoform expression in hematopoietic lineage choice. Genes Dev. 17 (8), 959–964. https://doi.org/10.1101/gad.251903.

Canesi, L., Gallo, G., Gavioli, M., Pruzzo, C., 2002. Bacteria–hemocyte interactions and phagocytosis in marine bivalves. Microsc. Res. Tech. 57 (6), 469–476. https://doi.org/10.1002/jemt.10100.

Chagraoui, H., Kristiansen, M.S., Ruiz, J.P., Serra-Barros, A., Richter, J., Hall-Ponsele, E., Gray, N., Waithe, D., Clark, K., Hublitz, P., Repapi, E., Otto, G., Sopp, P., Taylor, S., Thongjuea, S., Vyas, P., Porcher, C., 2018. SCL/TAL1 cooperates with Polycomb RYBP-PRC1 to suppress alternative lineages in blood-fated cells. Nat. Commun. 9 https://doi.org/10.1038/s41467-018-07787-6.

Clark, M.S., Peck, L.S., Arivalagan, J., Backeljau, T., Berland, S., Cardoso, J.C.R., Caurcel, C., Chapelle, G., De Noia, M., Dupont, S., Gharbi, K., Hoffman, J.I., Last, K. S., Marie, A., Melzner, F., Michalek, K., Morris, J., Power, D.M., Ramesh, K., Sanders, T., Sillanpää, K., Sleight, V.A., Stewart-Sinclair, P.J., Sundell, K., Telesca, L., Vendrami, D.L.J., Ventura, A., Wilding, T.A., Yarra, T., Harper, E.M., 2020. Deciphering mollusc shell production: the roles of genetic mechanisms through to ecology, aquaculture and biomimetics. Biol. Rev. 95 (6), 1812–1837. https://doi.org/10.1111/brv.12640.

Debnath, S., Jaako, P., Siva, K., Rothe, M., Chen, J., Dahl, M., Gaspar, H.B., Flygare, J., Schambach, A., Karlsson, S., 2017. Lentiviral vectors with cellular promoters correct Anemia and lethal B one marrow failure in a mouse model for diamond-Blackfan Anemia. Mol. Therapy: J. Am. Soc. Gene Therapy 25 (8), 1805–1814. https://doi.org/10.1016/j.ymthe.2017.04.002.

Dey, S., Curtis, D.J., Jane, S.M., Brandt, S.J., 2010. The TAL1/SCL transcription factor regulates cell cycle progression and proliferation in differentiating murine bone marrow monocyte precursors. Mol. Cell. Biol. 30 (9), 2181–2192. https://doi.org/10.1128/MCB.01441-09.

Drake, C.J., Fleming, P.A., 2000. Vasculogenesis in the day 6.5 to 9.5 mouse embryo. Blood 95 (5), 1671–1679. https://doi.org/10.1182/blood.V95.5.1671.005k39_1671_1679.

El Omari, K., Hoosdally, S.J., Tuladhar, K., Karia, D., Hall-Ponsele, E., Platonova, O., Vyas, P., Patient, R., Porcher, C., Mancini, E.J., 2013. Structural basis for LMO2-driven recruitment of the SCL:E47bHLH heterodimer to hematopoietic-specific transcriptional targets. Cell Rep. 4 (1), 135–147. https://doi.org/10.1016/j.celrep.2013.06.008.

Fan, S., Li, X., Guo, X., Zhang, R., Chen, Y., Zhao, F., Zhang, L., Qin, Z., Zhang, Z., 2024. Examination of the role of a novel transcription factor in activating Foxl2 and its potential involvement in the regulation of ovarian development in scallops. Aquaculture 578, 740113. https://doi.org/10.1016/j.aquaculture.2023.740113.

Fire, A., Xu, S., Montgomery, M.K., Kostas, S.A., Driver, S.E., Mello, C.C., 1998. Potent and specific genetic interference by double-stranded RNA in Caenorhabditis elegans. Nature 391 (6669), 806–811. https://doi.org/10.1038/35888.

Fujiwara, T., Alqadi, Y.W., Okitsu, Y., Fukuhara, N., Onishi, Y., Ishizawa, K., Harigae, H., 2013. Role of transcriptional corepressor ETO2 in erythroid cells. Exp. Hematol. 41 (3), 303–315.e301. https://doi.org/10.1016/j.exphem.2012.10.015.

Goardon, N., Lambert, J.A., Rodriguez, P., Nissaire, P., Herblot, S., Thibault, P., Dumenil, D., Strouboulis, J., Romeo, P.-H., Hoang, T., 2006. ETO2 coordinates cellular proliferation and differentiation during erythropoiesis. EMBO J. 25 (2), 357–366. https://doi.org/10.1038/sj.emboj.7600934.

Gu, X., Qiao, X., Yu, S., Song, X., Wang, L., Song, L., 2022. Histone lysine-specific demethylase 1 regulates the proliferation of hemocytes in the oyster Crassostrea gigas. Front. Immunol. 13, 1088149 https://doi.org/10.3389/fimmu.2022.1088149.

Hoang, T., Lambert, J.A., Martin, R., 2016. SCL/TAL1 in hematopoiesis and cellular reprogramming. In: Bresnick, E.H. (Ed.), Hematopoiesis, pp. 163–204.

Hu, Y., Stilp, A.M., McHugh, C.P., Rao, S., Jain, D., Zheng, X., Lane, J., Méric de Bellefon, S., Raffield, L.M., Chen, M.-H., Yanek, L.R., Wheeler, M., Yao, Y., Ren, C., Broome, J., Moon, J.-Y., de Vries, P.S., Hobbs, B.D., Sun, Q., Surendran, P., Brody, J. A., Blackwell, T.W., Choquet, H., Ryan, K., Duggirala, R., Heard-Costa, N., Wang, Z., Chami, N., Preuss, M.H., Min, N., Ekunwe, L., Lange, L.A., Cushman, M., Faraday, N., Curran, J.E., Almasy, L., Kundu, K., Smith, A.V., Gabriel, S., Rotter, J.I., Fornage, M., Lloyd-Jones, D.M., Vasan, R.S., Smith, N.L., North, K.E., Boerwinkle, E., Becker, L.C., Lewis, J.P., Abecasis, G.R., Hou, L., O'Connell, J.R., Morrison, A.C., Beaty, T.H., Kaplan, R., Correa, A., Blangero, J., Jorgenson, E., Psaty, B.M., Kooperberg, C., Walton, R.T., Kleinstiver, B.P., Tang, H., Loos, R.J.F., Soranzo, N., Butterworth, A.S., Nickerson, D., Rich, S.S., Mitchell, B.D., Johnson, A.D., Auer, P.L., Li, Y., Mathias, R. A., Lettre, G., Pankratz, N., Laurie, C.C., Laurie, C.A., Bauer, D.E., Conomos, M.P., Reiner, A.P., Consortium, N.T.-O.F.P.M, 2021. Whole-genome sequencing association analysis of quantitative red blood cell phenotypes: the NHLBI TOPMed program. Am. J. Hum. Genet. 108 (6), 1165. https://doi.org/10.1016/j.ajhg.2021.04.015.

Hung, C.H., Lee, T.L., Huang, A.Y.S., Yang, K.C., Shyu, Y.C.A., Wen, S.C., Lu, M.J., Yuan, S.S., Shen, C.K.J., 2021. A positive regulatory feedback loop between EKLF/KLF1 and TAL1/SCL sustaining the erythropoiesis. Int. J. Mol. Sci. 22 (15) https://doi.org/10.3390/ijms22158024.

Jemaà, M., Morin, N., Cavelier, P., Cau, J., Strub, J.-M., Delsert, C., 2014. Adult somatic progenitor cells and hematopoiesis in oyster. J. Exp. Biol. https://doi.org/10.1242/jeb.106575.

Jia, Z., Jiang, S., Wang, M., Wang, X., Liu, Y., Lv, Z., Song, X., Li, Y., Wang, L., Song, L., 2021. Identification of a novel pattern recognition receptor DM9 domain containing protein 4 as a marker for pro-Hemocyte of Pacific oyster Crassostrea gigas. Front. Immunol. 11 https://doi.org/10.3389/fimmu.2020.603270.

Jin, H., Liu, H., Wang, J., Zhang, W., Bao, Y., 2023a. CBFA2T3 affects red blood phenotype in the blood clam Tegillarca granosa by regulating hemocyte proliferation. Aquaculture, 740462. https://doi.org/10.1016/j.aquaculture.2023.740462.

Jin, H., Zhang, W., Liu, H., Bao, Y., 2023b. Genome-wide identification and characteristic analysis of ETS gene family in blood clam Tegillarca granosa. BMC Genomics 24 (1). https://doi.org/10.1186/s12864-023-09731-5.

Leong, W.Z., Tan, S.H., Ngoc, P.C.T., Amanda, S., Yam, A.W.Y., Liau, W.S., Gong, Z.Y., Lawton, L.N., Tenen, D.G., Sanda, T., 2017. ARID5B as a critical downstream target of the TAL1 complex that activates the oncogenic transcriptional program and promotes T-cell leukemogenesis. Genes Dev. 31 (23–24), 2343–2360. https://doi.org/10.1101/gad.302646.117.

Letunic, I., Bork, P., 2021. Interactive tree of life (iTOL) v5: an online tool for phylogenetic tree display and annotation. Nucleic Acids Res. 49 (W1), W293–W296. https://doi.org/10.1093/nar/gkab301.

Mansour, M.R., Sanda, T., Lawton, L.N., Li, X.Y., Kreslavsky, T., Novina, C.D., Brand, M., Gutierrez, A., Kelliher, M.A., Jamieson, C.H.M., von Boehmer, H., Young, R.A., Look, A.T., 2013. The TAL1 complex targets the FBXW7 tumor suppressor by activating miR-223 in human T cell acute lymphoblastic leukemia. J. Exp. Med. 210 (8), 1545–1557. https://doi.org/10.1084/jem.20122516.

McDonough, E.M., Barrett, C.W., Bradley, A., Choksi, Y.A., Ning, W., Poindexter, S., Parang, B., Fischer, M., Chaturvedi, R., Revetta, F., Washington, K., Hiebert, S.W., Wilson, K.T., Williams, C.S., 2012. MTG16 functions as a tumor suppressor in murine inflammatory carcinogenesis. Gastroenterology 142 (5), S27.

Michelson, A.M., 2008. Developmental biology. From genetic association to genetic switch. Science (New York, N.Y.) 322 (5909), 1803–1804. https://doi.org/10.1126/science.1169216.

Nain, N., Singh, A., Khan, S., Kaushik, M., Kukreti, S., 2022. Structural switching/polymorphism by sequential base substitution at quasi-palindromic SNP site (G → a) in LCR of human β-globin gene cluster. Int. J. Biol. Macromol. 201, 216–225. https://doi.org/10.1016/j.ijbiomac.2021.12.142.

Outman, A., Deracinois, B., Flahaut, C., Diab, M.A., Dhaouefi, J., Gressier, B., Eto, B., Nedjar, N., 2023. Comparison of the bioactive properties of human and bovine hemoglobin hydrolysates obtained by enzymatic hydrolysis: antimicrobial and antioxidant potential of the active peptide α137-141. Int. J. Mol. Sci. 24 (17), 13055 https://doi.org/10.3390/ijms241713055.

Palii, C.G., Perez-Iratxeta, C., Yao, Z.Z., Cao, Y., Dai, F.T., Davison, J., Atkins, H., Allan, D., Dilworth, F.J., Gentleman, R., Tapscott, S.J., Brand, M., 2011. Differential genomic targeting of the transcription factor TAL1 in alternate haematopoietic lineages. EMBO J. 30 (3), 494–509. https://doi.org/10.1038/emboj.2010.342.

Porcher, C., Chagraoui, H., Kristiansen, M.S., 2017. SCL/TAL1: a multifaceted regulator from blood development to disease. Blood 129 (15), 2051–2060. https://doi.org/10.1182/blood-2016-12-754051.

Rojas-Sutterlin, S., Lecuyer, E., Hoang, T., 2014. Kit and Scl regulation of hematopoietic stem cells. Curr. Opin. Hematol. 21 (4), 256–264. https://doi.org/10.1097/moh.0000000000000052.

Ronquist, F., Teslenko, M., van der Mark, P., Ayres, D.L., Darling, A., Höhna, S., Larget, B., Liu, L., Suchard, M.A., Huelsenbeck, J.P., 2012. MrBayes 3.2: efficient Bayesian phylogenetic inference and model choice across a large model space. Syst. Biol. 61 (3), 539–542. https://doi.org/10.1093/sysbio/sys029.

Rozewicki, J., Li, S., Amada, K.M., Standley, D.M., Katoh, K., 2019. MAFFT-DASH: integrated protein sequence and structural alignment. Nucleic Acids Res. 47 (W1), W5–W10. https://doi.org/10.1093/nar/gkz342.

Ryan, D.P., Duncan, J.L., Lee, C., Kuchel, P.W., Matthews, J.M., 2007. Assembly of the oncogenic DNA-binding complex LMO2-Ldb1-TAL1-E12. Proteins: Struct., Funct., Bioinf. 70 (4), 1461–1474. https://doi.org/10.1002/prot.21638.

Sankaran, V.G., Xu, J., Orkin, S.H., 2010. Transcriptional silencing of fetal hemoglobin by BCL11A. Ann. N. Y. Acad. Sci. 1202 (1), 64–68. https://doi.org/10.1111/j.1749-6632.2010.05574.x.

Schindelin, J., Arganda-Carreras, I., Frise, E., Kaynig, V., Longair, M., Pietzsch, T., Preibisch, S., Rueden, C., Saalfeld, S., Schmid, B., Tinevez, J.-Y., White, D.J., Hartenstein, V., Eliceiri, K., Tomancak, P., Cardona, A., 2012. Fiji: an open-source platform for biological-image analysis. Nat. Methods 9 (7), 676–682. https://doi.org/10.1038/nmeth.2019.

Shibata, M., Nagai, K., Doi, T., Tawada, H., Taniguchi, S., 2012. Blood color is influenced by inflammation and independently predicts survival in hemodialysis patients: quantitative evaluation of blood color. Artif. Organs 36 (11), 992–998. https://doi.org/10.1111/j.1525-1594.2012.01490.x.

Song, L., Wang, L., Qiu, L., Zhang, H., 2010. Bivalve immunity. Adv. Exp. Med. Biol. 708, 44–65. https://doi.org/10.1007/978-1-4419-8059-5_3.

Song, X., Song, Y., Dong, M., Liu, Z., Wang, W., Wang, L., Song, L., 2019. A new member of the runt domain family from Pacific oyster Crassostrea gigas (CgRunx) potentially involved in immune response and larvae hematopoiesis. Fish Shellfish Immunol. 89, 228–236. https://doi.org/10.1016/j.fsi.2019.03.066.

Song, X.R., Wang, H., Chen, H., Sun, M.Z., Liang, Z.X., Wang, L.L., Song, L.S., 2016. Conserved hemopoietic transcription factor cg-SCL delineates hematopoiesis of Pacific oyster Crassostrea gigas. Fish Shellfish Immunol. 51, 180–188. https://doi.org/10.1016/j.fsi.2016.02.023.

Steinauer, N., Guo, C., Zhang, J.S., 2017. Emerging roles of MTG16 in cell-fate control of hematopoietic stem cells and Cancer. Stem Cells Int. 2017 https://doi.org/10.1155/2017/6301385.

Sun, B., Zhang, P., Wei, H., Jia, R., Huang, T., Li, C., Yang, W., 2022. Effect of hemoglobin extracted from Tegillarca granosa on iron deficiency anemia in mice. Food Res. Intern. (Ottawa, Ont.) 162 (Pt A), 112031. https://doi.org/10.1016/j.foodres.2022.112031.

Sun, C.-W., Wu, L.-C., Knopick, P.L., Bradley, D.S., Townes, T., Terman, D.S., 2017. Sickle cells produce functional immune modulators and cytotoxics. Am. J. Hematol. 92 (10), 981–988. https://doi.org/10.1002/ajh.24836.

Tan, T.K., Zhang, C.J., Sanda, T., 2019. Oncogenic transcriptional program driven by TAL1 in T-cell acute lymphoblastic leukemia. Int. J. Hematol. 109 (1), 5–17. https://doi.org/10.1007/s12185-018-2518-z.

Taniguchi, C.N., Dobbs, J., Dunn, M.A., 2017. Heme iron, non-heme iron, and mineral content of blood clams (Anadara spp.) compared to Manila clams (V. Philippinarum), Pacific oysters (C. Gigas), and beef liver (B. Taurus). J. Food Compos. Anal. 57, 49–55. https://doi.org/10.1016/j.jfca.2016.12.018.

Toscano, M.G., Navarro-Montero, O., Ayllon, V., Ramos-Mejia, V., Guerrero-Carreno, X., Bueno, C., Romero, T., Lamolda, M., Cobo, M., Martin, F., Menendez, P., Real, P.J., 2015. SCL/TAL1-mediated transcriptional network enhances megakaryocytic specification of human embryonic stem cells. Mol. Ther. 23 (1), 158–170. https://doi.org/10.1038/mt.2014.196.

Vagapova, E.R., Spirin, P.V., Lebedev, T.D., Prassolov, V.S., 2018. The role of TAL1 in hematopoiesis and Leukemogenesis. Acta Nat. 10 (1), 15–23. https://doi.org/10.32607/20758251-2018-10-1-15-23.

Wang, S., Yu, X., Zhang, S., Jin, H., Chen, Z., Lin, Z., Bao, Y., 2021. Cu2+ inhibits the peroxidase and antibacterial activity of homodimer hemoglobin from blood clam Tegillarca granosa by destroying its Heme pocket structure. Front. Mar. Sci. 8 https://doi.org/10.3389/fmars.2021.635210.

Wu, R., Zhang, Q., Li, Y., 2020. Development, characterization of monoclonal antibodies specific for the ORF25 membrane protein of cyprinid herpesvirus 2 and their applications in immunodiagnosis and neutralization of virus infection. Aquaculture 519. https://doi.org/10.1016/j.aquaculture.2019.734904.

Xu, W., Jin, S., Su, H., Tran, N.-T., Song, J., Lu, S.S., Li, Y., Huang, S., Abdel-Wahab, O., Liu, Y., Zhao, X., 2017. Splicing factor SF3B1K700E mutant dysregulates erythroid differentiation via aberrant alternative splicing of transcription factor TAL1. PLoS One 12 (5). https://doi.org/10.1371/journal.pone.0175523.

Yamada, Y., Zhong, Y., Miki, S., Taura, A., Rabbitts, T.H., 2022. The transcription factor complex LMO2/TAL1 regulates branching and endothelial cell migration in sprouting angiogenesis. Sci. Rep.-Uk 12 (1). https://doi.org/10.1038/s41598-022-11297-3.

Yan, H., Ali, A., Blanc, L., Narla, A., Lane, J.M., Gao, E., Papoin, J., Hale, J., Hillyer, C.D., Taylor, N., Gallagher, P.G., Raza, A., Kinet, S., Mohandas, N., 2021. Comprehensive phenotyping of erythropoiesis in human bone marrow: evaluation of normal and ineffective erythropoiesis. Am. J. Hematol. 96 (9), 1064–1076. https://doi.org/10.1002/ajh.26247.

Yang, Z., He, X., Jin, H., Su, D., Lin, Z., Liu, H., Bao, Y., 2023. Hemocyte proliferation is associated with blood color shade variation in the blood clam, *Tegillarca granosa*. Aquaculture, 739447. https://doi.org/10.1016/j.aquaculture.2023.739447.

Yu, J., Teng, S., Yue, X., Wang, H., Liu, B., 2023. The toll pathway and Duox-ROS system are required for the clam antibac terial immune response in the hepatopancreas. Aquaculture 574, 739637. https://doi.org/10.1016/j.aquaculture.2023.739637.

Zhang, N., Pan, L., Liao, Q., Tong, R., Li, Y., 2023. Potential molecular mechanism underlying the harmed haemopoiesis upon benzo[a]pyrene exposure in Chlamys farreri. Fish Shellfish Immunol. 141 https://doi.org/10.1016/j.fsi.2023.109032.

Zhang, W., Yin, F., Bao, Y., 2021. Genome-wide identification and characterization of basic helix-loop-helix genes in nine molluscs. Gene 785, 145604. https://doi.org/10.1016/j.gene.2021.145604.